

A TWO ZONE SYNCHROTRON MODEL FOR THE KNOTS IN THE M87 JET

S. Sahayanathan*

Astrophysical Sciences Division, Bhabha Atomic Research Centre, Mumbai - 400085, India

26 March 2021

ABSTRACT

The flux and the spectral index in X-ray energy band from the knots of M87 jet as observed by *Chandra* indicate a possible synchrotron origin but cannot be explained by simple one zone models with continuous injection of non-thermal electrons. In this letter we propose a two-zone model to explain the observed spectra of the knots of M87 jet. We consider the synchrotron emission from a region with tangled magnetic field where relativistic non-thermal electrons are continuously injected in from an associated acceleration region. The acceleration region is assumed to be compact zone possibly around a shock front. A power-law distribution of electron is injected into the acceleration region and are accelerated to a maximum energy determined by the acceleration time scale and the loss processes. With the present model we are able to explain the overall broadband features of the knots of M87 jet. Also the present model predicts a change in spectral index at ultraviolet energies and future observations at these energies can be used to constrain the parameters involved in the model.

Key words: galaxies: active - galaxies: individual(M87) - galaxies: jets - X-rays: galaxies

1 INTRODUCTION

M87 is a nearby giant elliptical galaxy (distance = 16 Mpc [Tonry (1991)]) possessing a one-sided jet with projected distance ≈ 2 Kpc and bright in radio, optical and X-ray energies. The jet structure is very well studied in radio (Owen et al. (1989); Biretta et al. (1995); Sparks et al. (1996)), IR (Perlman et al. (2001); Sparks et al. (1996)) and optical (Meisenheimer et al. (1996); Sparks et al. (1996)) bands. Prior to *Chandra*, M87 jet was not very well studied at X-ray energies due to the limited angular resolution of earlier X-ray telescopes, *Einstein* and ROSAT. However, *Chandra* due to its better spatial resolution is able to resolve many fainter knots of M87 jet which are observed only in radio and optical bands earlier. Moreover, the position of these knots in X-ray energies are nearly coincident with their radio/optical counterparts(Perlman et al. (2001); Perlman & Wilson (2005)). Also M87 is the only radio-galaxy (other than CenA(Sreekumar et al. (1999))) which is detected in GeV-TeV energies(Aharonian et al. (2003)). Initially it was not well understood whether the TeV gamma-ray emission region is close to nucleus(Georganopoulos et al. (2005)) or from the knot HST-1(Stawarz et al. (2006)). However the detection of M87 by HESS confirmed the

high energy emission from the region close to the nucleus(Aharonian et al. (2006)). Recent VERITAS detection of VHE emission from M87 (Benbow (2008)) again suggests the emission may not be from HST-1¹. Considering the fact M87 jet is misaligned to the observer, explaining this TeV gamma-ray emission required a modified model other than the one used to explain blazar emission. Neronov & Aharonian (2007) explained TeV gamma-ray emission due to radiative cooling of electrons accelerated by strong rotation induced electric fields in the vacuum gaps in black hole magnetospheres. Lenain et al. (2008) proposed a multi-blob model with several plasma blobs moving in the large opening angle of the jet formation zone. TeV gamma-ray emission is explained as Doppler boosted synchrotron self Compton radiation by the blobs moving close to the line of sight.

The radio-to-optical emission from the knots of M87 jet are quite well accepted as synchrotron emission due to cooling of relativistic non-thermal electrons by the magnetic field therein(Perlman et al. (2001)). The flux and the spectral indices at X-ray energies indicates a possible continuation of synchrotron emission of the radio-to-optical spec-

* E-mail: sunder@barc.gov.in

¹ <http://polywww.in2p3.fr/actualites/congres/blazars2008>

tra with the change in the spectral index beyond optical energies (Marshall et al. (2002), Stawarz et al. (2005)).

Simple theoretical models viz. continuous injection model (hereafter CI) (Kardashev (1962); Ginzburg & Syrovatskii (1968); Heavens & Meisenheimer (1987); Meisenheimer et al. (1989)) and one time injection model (Jaffe & Perola (1973); Kardashev (1962); Pacholczyk (1970)) were unable to explain the observed X-ray flux and/or the spectral index. The CI model considers the synchrotron emission from non-thermal electrons injected continuously into a region with tangled magnetic field. But the X-ray flux predicted by this model is more than the observed flux (Perlman & Wilson (2005)). In one time injection model, a burst of electrons are injected at $t = 0$ and allowed to evolve with (Jaffe & Perola (1973)) or without pitch angle scattering (Kardashev (1962); Pacholczyk (1970)). The model with pitch angle scattering under predicts the X-ray flux and the one without pitch angle scattering fail to predict the observed X-ray spectral index (Perlman & Wilson (2005)). However CI and one time injection models are able to reproduce the broadband spectra of the knots of various AGN detected by *Chandra* (Sahayanathan et al. (2003); Sambruna et al. (2002)).

In this letter we propose a two zone model to explain the non-thermal emission from the knots of M87 jet. We consider a situation where a power-law distribution of electrons are accelerated by an shock. The initial particle spectrum which is accelerated by the shock can be an outcome of an earlier acceleration process. The particles accelerated by the shock cool via synchrotron radiation in a homogeneous magnetic field behind it. The present model is similar to a situation where particles accelerated by an external shock are advected downstream to be accelerated further by an internal shock. Two zone models were in fact used by various authors to explain the spectral and the temporal behaviour of blazars (Kirk et al. (1998); Bhattacharyya et al. (2005); Li & Kusunose (2000)). In the next section, the formulation of the present model and the parameters involved are discussed. In §3 we discuss the results of the fitting using the present model and compare the present model with the other existing models.

2 THE TWO ZONE MODEL

We consider the acceleration of a power-law distribution of particles (which may be a relic of past acceleration process) at a shock front and cool via synchrotron radiation in a homogeneous magnetic field. We treat the present scenario as a two zones: one around the shock front where the particles are accelerated (AR) and downstream region where they loose most of their energy through synchrotron process (CR). This model is then used to explain the radio-optical-X-radio spectra of the knots in M87 jet. We assume the CR to be a spherical blob of radius R with tangled magnetic field B_{CR} and AR is assumed to be a very thin region with magnetic field B_{AR} . Power law distribution of electrons are continuously injected into AR and are accelerated by the shock characterized by an acceleration timescale t_{acc} . Particles are then accelerated at an rate $1/t_{acc}$ to a maximum energy determined by the loss processes. AR is assumed to

be compact and the emission from CR mainly contributes the overall photon spectrum.

The kinetic equation governing the evolution of electrons in AR is given by

$$\frac{\partial n(\gamma, t)}{\partial t} = \frac{\partial}{\partial \gamma} \left[\left(\beta_{AR} \gamma^2 - \frac{\gamma}{t_{acc}} \right) n(\gamma, t) \right] - \frac{n(\gamma, t)}{t_{esc}} + Q(\gamma) \quad (1)$$

Where

$$Q(\gamma) d\gamma = q_o \gamma^{-p} d\gamma \quad \text{for } \gamma_{min} < \gamma < \gamma_b \quad (2)$$

Here γ is the Lorentz factor of the electron, t_{esc} is the escape timescale and $\beta_{AR} = \frac{\sigma_T}{6\pi mc} B_{AR}^2$.

Equation (1) can be solved analytically using Green's function (Atoyan & Aharonian (1999)) and the electron distribution for an energy-independent t_{acc} and t_{esc} at time t is given by

$$n(\gamma, t) = t_{acc} \gamma^{-(\alpha+1)} \left(1 - \frac{\gamma}{\gamma_{max}} \right)^{\alpha-1} \int_{x_o}^{\gamma} Q(x) \left[\frac{1}{x} - \frac{1}{\gamma_{max}} \right]^{-\alpha} dx \quad (3)$$

Where $\alpha = t_{acc}/t_{esc}$ and the lower limit of integration x_o is given by

$$x_o = \left[\frac{1}{\gamma_{max}} + \left(\frac{1}{\gamma} - \frac{1}{\gamma_{max}} \right) \exp(t/t_{acc}) \right]^{-1} \quad (4)$$

$\gamma_{max} = 1/(\beta_{AR} t_{acc}) > \gamma_b$ is the maximum Lorentz factor an electron can attain in AR. For $t \gg t_{acc}$ equation (4) can be approximated to be γ_{min} as the injection term in equation (3) vanishes for $x < \gamma_{min}$.

The evolution of the electrons in CR is governed by the equation

$$\frac{\partial N(\gamma, t)}{\partial t} = \frac{\partial}{\partial \gamma} [\beta_{CR} \gamma^2 N(\gamma, t)] + Q_{AR}(\gamma) \quad (5)$$

Here the last term is the injection from AR $Q_{AR}(\gamma) = n(\gamma)/t_{esc}$ and for $t \gg t_{acc}$

$$Q_{AR}(\gamma) \approx q_o \alpha \gamma^{-(\alpha+1)} \left(1 - \frac{\gamma}{\gamma_{max}} \right)^{\alpha-1} \int_{\gamma_{min}}^{MIN(\gamma, \gamma_b)} x^{-p} \left[\frac{1}{x} - \frac{1}{\gamma_{max}} \right]^{-\alpha} dx \quad (6)$$

and $\beta_{CR} = \frac{\sigma_T}{6\pi mc} B_{CR}^2$.

The distribution of electron at time t in CR from equation (5) is given by

$$N(\gamma, t) = \frac{1}{\beta_{CR} \gamma^2} \int_{\gamma}^{\Gamma_o} Q_{AR}(x) dx \quad (7)$$

Where $\Gamma_o = \gamma/(1 - \gamma\beta_{CR}t)$.

From equation (3), it can be shown that the injection into CR (for $\alpha + 1 > p$) is a broken power-law with index $-p$ for $\gamma < \gamma_b$ and $-(\alpha + 1)$ for $\gamma > \gamma_b$. The synchrotron losses in CR introduces an additional break γ_c in the electron spectrum depending upon the age of CR (t_{obs}) and the B_{CR} .

$$\gamma_c = \frac{1}{\beta_{CR} t_{obs}} \quad (8)$$

The electron spectrum in CR at t_{obs} can then have two different spectral shapes depending on the location of γ_c with respect to γ_b .

(i) $\gamma_c > \gamma_b$: The final spectrum will have two breaks with indices

$$N(\gamma, t_{obs}) \propto \begin{cases} \gamma^{-p}, & \gamma_{min} < \gamma < \gamma_b \\ \gamma^{-(\alpha+1)}, & \gamma_b < \gamma < \gamma_c \\ \gamma^{-(\alpha+2)}, & \gamma_c < \gamma < \gamma_{max} \end{cases} \quad (9)$$

(ii) $\gamma_c < \gamma_b$: In this case the indices are

$$N(\gamma, t_{obs}) \propto \begin{cases} \gamma^{-p}, & \gamma_{min} < \gamma < \gamma_c \\ \gamma^{-(p+1)}, & \gamma_c < \gamma < \gamma_b \\ \gamma^{-(\alpha+2)}, & \gamma_c < \gamma < \gamma_{max} \end{cases} \quad (10)$$

The synchrotron emissivity ϵ_ν from the resultant electron spectrum is then calculated by convoluting $N(\gamma, t)$ with single particle emissivity averaged over an isotropic distribution of pitch angles $P(\nu, \gamma)$

$$\epsilon_\nu = \frac{1}{4\pi} \int_1^\infty N(\gamma, t) P(\nu, \gamma) d\gamma \quad (11)$$

The predicted spectrum by the above model depends on nine parameters, which are q_o , α , γ_{min} , γ_b , γ_{max} , p , B_{CR} , R and t_{obs} . Here α and p are estimated from the radio-to-optical and optical-to-X-ray spectral indices, q_o and B_{CR} are constrained using the observed luminosity and equipartition magnetic field. For R we assume the physical sizes measured in radio (Hardee (1982)). Age of the knot t_{obs} is chosen to introduce a break in the observed spectrum at optical band and γ_b is fitted to reproduce the observed X-ray flux. γ_{min} and γ_{max} are used as free parameters and are fixed at 5 and 10^8 .

3 RESULTS AND DISCUSSION

We applied the above model to explain the knots D, F, A and B of M87 jet and the results of the fitting are shown in Figure 1 and the parameters used for the fit are given in Table 1. The spectrum of knot E can be explained by simple CI model and the parameters we quote corresponds to CI model. We did not model knot C due to significant differences in X-ray-optical properties(Perlman & Wilson (2005)).

For all the fits shown in Figure 1, $\gamma_c < \gamma_b$. However, one can fit the spectrum with $\gamma_c > \gamma_b$ with proper choices of the parameters α , γ_b and γ_c . This degeneracy arises due to the unavailability of UV spectral index since the present model predicts the corresponding particle spectral index as $-(\alpha+1)$ or $-(p+1)$ (equation (9) and (10)) depending upon the above two conditions. Future observations at these photon energies may help in validating the present model and also will remove this degeneracy. Also, to obtain a precise values for p and α , spectral indices at radio-optical and X-ray energies should be known accurately. In general t_{acc} and t_{esc} can be energy dependent and in such a situation the solution (equation (3)) may differ from its form and the index beyond γ_b may not be the one discussed above.

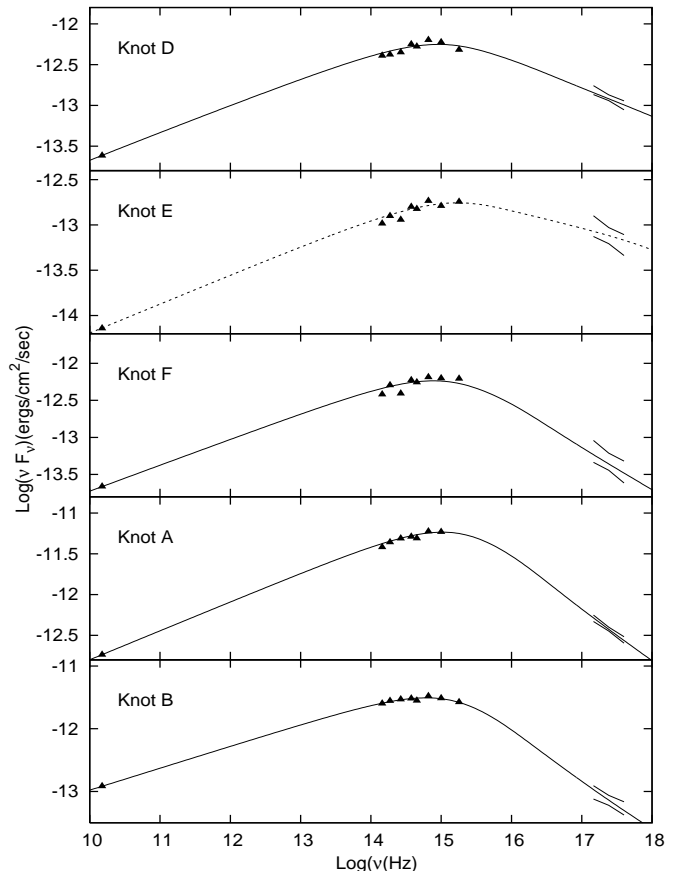


Figure 1. The spectral fit of the present model with the observed fluxes in radio(Perlman et al.(2001)), optical(Perlman et al.(2001), Waters & Zepf(2005)) and X-ray((Perlman & Wilson(2005))). The observed spectra of Knot E is fitted with CI model (dashed line). Errors in radio and optical are too small to be seen and hence not shown in the figure.

Using the present model we estimated the flux at GeV-TeV energies due to inverse Compton scattering and are given in Table 1. For the inverse Compton process the target photon can be either synchrotron photon(SSC) or cosmic microwave background radiation(IC/CMBR) or both. From the observed superluminal velocities of $2c$ to $6c$ and the viewing angle of 10° to 20° (Biretta et al. (1999)) we found the synchrotron photon energy density dominates over the Doppler boosted cosmic microwave background radiation. Hence the flux quoted in Table 1 are due to SSC process and are below the sensitivity of the present gamma-ray telescopes *MAGIC*(Majumdar & et al. (2005)), *HESS* and the upcoming experiment *GLAST*². Hence discrimination of the models based on GeV-TeV observations as discussed in Georganopoulos et al. (2006) for 3C273 cannot be done for M87 jets.

A possible scenario of the present model is where AR is a region around an internal shock following an external shock. The electron injection into AR can be the one which are already accelerated by an external shock and are

² <http://www-glast.slac.stanford.edu/>

advected downstream to be accelerated further by the internal shock (Tammi & Dempsey (2007); Pope & Melrose (1994)). An internal shock description for the knots in AGN jets has already been discussed in literature (Rees (1978); Sahayanathan & Misra (2005)). Alternatively, reacceleration of power law electron distribution by turbulence at boundary shear layers can also be another possible scenario (De Young (1986); Stawarz & Ostrowski (2003)). Inclusion of these scenario in its exact form into the present model will make it more complex and is beyond the scope of the present work.

Perlman & Wilson (2005) proposed a modified CI model where the volume within which particle acceleration occurs is energy-dependent. This is expressed in terms of a filling factor f_{acc} which is the ratio between the observed flux to the flux predicted by the simple CI model. They found f_{acc} declining with increasing distance from the nucleus suggesting particle acceleration taking place in larger fraction of the jet volume in the inner jet than the outer jet. The energy dependence of f_{acc} also indicates that particle acceleration regions occupy a smaller fraction of jet volume at higher energies. Even though the model is phenomenological, it indicates that the process of high energy emission from the knots are as complicated as their physical region. However the mechanism responsible for the filling factor is not explained.

Stawarz et al. (2006) explained the knot HST-1 of M87 jet as a region when the reconfinement shock reaches the jet axis. They considered at the initial stage of M87 jet, the particles expand freely decreasing the pressure rapidly than the ambient gas pressure. This will develop (in case of M87) a reconfinement shock which reaches the jet axis at a location which coincide with that of the knot HST-1. They postulate this location as the beginning of HST-1 and while its outer parts are identified as stationary reflected shock formed when the reconfinement shock reaches the jet axis. Also they evaluated the ambient radiation field along the jet axis and estimated the TeV gamma-ray emission from HST-1 initiated by an outburst experienced at the core. Since the reconfinement shock requires an initial free expansion, the knots downstream HST-1 cannot be explained by this model.

Fleishman (2006) explained the flattening of non-thermal spectra in the ultraviolet and X-ray bands observed from the knots of M87 and 3C273 jets through diffusive synchrotron radiation (DSR) in random small-scale magnetic fields. Whereas the synchrotron spectrum from regular large-scale magnetic field dominates the spectra at low energy band. The DSR spectrum at high energy is $\propto \omega^{-\nu}$ where ω is the observed photon frequency and ν is the spectral index of the random magnetic field assumed to be a power-law. Honda & Honda (2007) proposed a filamentary jet model to explain the observed X-ray spectral index. In their model, the jet comprises magnetic filaments of transverse size λ and particles trapped in this filaments are accelerated by diffusive shock acceleration. The acceleration of the electrons bound to a large filament are controlled by the radiative losses before escape from the filament. Whereas the electrons trapped in smaller filaments escape via energization. A critical scale λ_c discriminates between the large and small scale filaments. They considered a situation where the magnetic field is larger for filaments with larger size and

found the electron energy peaks when trapped in the filament of size λ_c . The X-ray spectrum is explained by the synchrotron radiation of the electrons accelerated in the filaments of size $\lambda > \lambda_c$. However, synchrotron radiation from large-scale magnetic field itself can reproduce the observed X-ray spectrum (present model) involving less number of parameters and/or assumptions (§2).

Recently Liu & Shen (2007) proposed a two zone model to explain the observed spectra of the knots of M87 jet. In their model electrons are accelerated to relativistic energies in acceleration region (AR) and loose most of their energies in cooling region (CR) through synchrotron process. They considered AR and CR are spatially separated and introduced a break in the particle spectrum injected in CR through the advection of particles from AR to CR. This along with the cooling break in CR produce a double broken power-law with indices $-p$, $-(p+1)$ and $-(p+2)$ which is then used to fit the observed spectra. However the present model assumes AR and CR are co-spatial supporting a more physical scenario where electrons accelerated by the shock, cools in its vicinity.

4 CONCLUSION

The observed radio-optical-X-ray spectra from the knots in the jets of the FRI radio galaxy M87 are explained within the framework of two zone model. We considered a power-law electron distribution which are further accelerated in an acceleration region and are injected into a cooling region where they lose their energy through synchrotron radiation. In its simplest form, the model does not consider any specific acceleration process but assumes an energy independent acceleration timescale. Future observations of M87 knots in UV-to-X-ray photon energies will confirm the present model and constrain the parameters involved.

We explored the possibility of the present model to reproduce the X-ray flux of other FRI galaxies (detected by *Chandra*) which are observed to have lower radio luminosity and relatively smaller jets when compared with FRII galaxies. The X-ray emission from FRI jet is quite well accepted to be of synchrotron origin whereas for FRII and quasars it may be due to IC/CMBR. However the latter is still under debate (see Harris & Krawczynski (2006) for a review about the X-ray emission from extragalactic jets). The X-ray emission from the knots and/or the jets of the FRI galaxies viz. 3C 66B (Hardcastle et al. (2001)), 3C 346 (Worrall & Birkinshaw (2005)), CenA (Hardcastle et al. (2006)) and 3C 296 (Hardcastle et al. (2005) listed in the online catalog of extragalactic X-ray jets XJET³, which are not explained by synchrotron emission from simple one zone models, can be reproduced by the present model.

The author thanks S. Bhattacharyya, N. Bhatt and M. Choudhury for the useful discussions and suggestions. The author is grateful to referee E. Perlman for useful comments and suggestions. This work has made use of the XJET website.

³ <http://hea-www.harvard.edu/XJET/>

Table 1. Model Parameters and Knot Properties

Knot	q_0	α	p	γ_b	B_{CR}	t_{obs}	γ_c	R	F_{1GeV} (photons/cm ² /s)	F_{50GeV} (photons/cm ² /s)	F_{1TeV} (photons/cm ² /s)
D	7.5	1.75	2.35	1.8	9.3	1.6	5.7	12	1.8×10^{-12}	3.7×10^{-14}	2.1×10^{-16}
E	4.7	...	2.36	...	5.9	2.5	9.0	17	1.7×10^{-13}	4.1×10^{-15}	4.6×10^{-17}
F	0.6	2.3	2.3	2.1	4.5	4.7	8.2	29	1.1×10^{-12}	2.6×10^{-14}	1.0×10^{-16}
A	1.0	2.45	2.29	2.0	4.7	3.5	10.1	55	2.3×10^{-11}	5.9×10^{-13}	2.1×10^{-15}
B	0.9	2.75	2.3	1.4	4.7	3.9	9.0	50	1.0×10^{-11}	2.3×10^{-13}	3.8×10^{-16}

Columns:- 1: Knot name. 2: Normalisation (in units of 10^{-12}) of the power-law injected into AR(for knot E it is the normalisation of the power-law injected into CR (see text)). 3: Ratio between the acceleration timescale and escape timescale in AR. 4: Index of the power-law spectrum injected into AR. 5: Maximum energy of the electron Lorentz factor injected into AR (in units of 10^6). 6: CR magnetic field (in units of 10^{-4} G). 7: Time of observation (in units of 10^9 sec). 8: Break Lorentz factor of the electrons due to synchrotron cooling in CR (in units of 10^5). 9: Size of CR (in parsec) measured in radio (Hardee (1982)). 10: Flux at 1GeV. 11: Flux at 50GeV. 12: Flux at 1TeV.

For all cases, the minimum Lorentz factor(γ_{min})injected into AR is 5 and maximum Lorentz factor(γ_{max}) attained in AR is 10^8 .

REFERENCES

- Aharonian, F., et al. 2003, A&A, 403, L1
 Aharonian, F., et al. 2006, Science, 314, 1424
 Atoyan, A. M., & Aharonian, F. A. 1999, MNRAS, 302, 253
 Benbow, W. 2008, Workshop on Blazar Variability, April 22-25, Palaiseau
 Bhattacharyya, S., Sahayanathan, S., & Bhatt, N. 2005, New Astronomy, 11, 17
 Biretta, J. A., Zhou, F., & Owen, F. N. 1995, ApJ, 447, 582
 Biretta, J. A., Sparks, W. B., & Macchetto, F. 1999, ApJ, 520, 621
 De Young, D. S. 1986, ApJ, 307, 62
 Fleishman, G. D. 2006, MNRAS, 365, L11
 Georganopoulos, M., Perlman, E. S., & Kazanas, D. 2005, ApJ, 634, L33
 Georganopoulos, M., Perlman, E. S., Kazanas, D., & McEnery, J. 2006, ApJ, 653, L5
 Ginzburg, V. L., & Syrovatskii, S. I. 1968, Ap&SS, 1, 442
 Hardee, P. E. 1982, ApJ, 261, 457
 Harris, D. E., & Krawczynski, H. 2006, ARAA, 44, 463
 Hardcastle, M. J., Birkinshaw, M., & Worrall, D. M. 2001, MNRAS, 326, 1499
 Hardcastle, M. J., Kraft, R. P., & Worrall, D. M. 2006, MNRAS, 368, L15
 Hardcastle, M. J., Worrall, D. M., Birkinshaw, M., Laing, R. A., & Bridle, A. H. 2005, MNRAS, 358, 843
 Heavens, A. F., & Meisenheimer, K. 1987, MNRAS, 225, 335
 Honda, M., & Honda, Y. S. 2007, ApJ, 654, 885
 Jaffe, W. J., & Perola, G. C. 1973, A&A, 26, 423
 Kardashev, N. S. 1962, Soviet Astronomy, 6, 317
 Kirk, J. G., Rieger, F. M., & Mastichiadis, A. 1998, A&A, 333, 452
 Lenain, J.-P., Boisson, C., Sol, H., & Katarzyński, K. 2008, A&A, 478, 111
 Li, H., & Kusunose, M. 2000, ApJ, 536, 729
 Liu, W.-P., & Shen, Z.-Q. 2007, ApJ, 668, L23
 Majumdar, P., & et al. 2005, International Cosmic Ray Conference, 5, 203
 Marshall, H. L., Miller, B. P., Davis, D. S., Perlman, E. S., Wise, M., Canizares, C. R., & Harris, D. E. 2002, ApJ, 564, 683
 Meisenheimer, K., Roser, H.-J., Hiltner, P. R., Yates, M. G., Longair, M. S., Chini, R., & Perley, R. A. 1989, A&A, 219, 63
 Meisenheimer, K., Roeser, H.-J., & Schloetelburg, M. 1996, A&A, 307, 61
 Neronov, A., & Aharonian, F. A. 2007, ApJ, 671, 85
 Owen, F. N., Hardee, P. E., & Cornwell, T. J. 1989, ApJ, 340, 698
 Pacholczyk, A. G. 1970, Series of Books in Astronomy and Astrophysics, San Francisco: Freeman, 1970,
 Perlman, E. S., Biretta, J. A., Sparks, W. B., Macchetto, F. D., & Leahy, J. P. 2001, ApJ, 551, 206
 Perlman, E. S., Sparks, W. B., Radomski, J., Packham, C., Fisher, R. S., Piña, R., & Biretta, J. A. 2001, ApJ, 561, L51
 Perlman, E. S., & Wilson, A. S. 2005, ApJ, 627, 140
 Pope, M. H., & Melrose, D. B. 1994, Proceedings of the Astronomical Society of Australia, 11, 175
 Rees, M. J. 1978, MNRAS, 184, 61P
 Sahayanathan, S., & Misra, R. 2005, ApJ, 628, 611
 Sahayanathan, S., Misra, R., Kembhavi, A. K., & Kaul, C. L. 2003, ApJ, 588, L77
 Sambruna, R. M., Maraschi, L., Tavecchio, F., Urry, C. M., Cheung, C. C., Chartas, G., Scarpa, R., & Gambill, J. K. 2002, ApJ, 571, 206
 Sparks, W. B., Biretta, J. A., & Macchetto, F. 1996, ApJ, 473, 254
 Sreekumar, P., Bertsch, D. L., Hartman, R. C., Nolan, P. L., & Thompson, D. J. 1999, Astroparticle Physics, 11, 221
 Stawarz, L., Aharonian, F., Kataoka, J., Ostrowski, M., Siemiginowska, A., & Sikora, M. 2006, MNRAS, 370, 981
 Stawarz, L., & Ostrowski, M. 2003, New Astronomy Review, 47, 521
 Stawarz, L., Siemiginowska, A., Ostrowski, M., & Sikora, M. 2005, ApJ, 626, 120
 Tammi, J., & Dempsey, P. 2007, ArXiv e-prints, 712, arXiv:0712.1749
 Tonry, J. L. 1991, ApJ, 373, L1
 Waters, C. Z., & Zepf, S. E. 2005, ApJ, 624, 656
 Worrall, D. M., & Birkinshaw, M. 2005, MNRAS, 360, 926